RESEARCH REPORT

Epigenetic changes occur at decidualisation genes as a function of reproductive ageing in mice

Laura Woods[1,2], Natasha Morgan[1,2], Xiang Zhao[3], Wendy Dean[3,4,5], Vicente Perez-Garcia[1,2] and Myriam Hemberger[1,2,4,5,6,*]

ABSTRACT

Reproductive decline in older female mice can be attributed to a failure of the uterus to decidualise in response to steroid hormones. Here, we show that normal decidualisation is associated with significant epigenetic changes. Notably, we identify a cohort of differentially methylated regions (DMRs), most of which gain DNA methylation between the early and late stages of decidualisation. These DMRs are enriched at progesterone-responsive gene loci that are essential for reproductive function. In female mice nearing the end of their reproductive lifespan, DNA methylation fidelity is lost at a number of CpG islands (CGIs) resulting in CGI hypermethylation at key decidualisation genes. Importantly, this hypermethylated state correlates with the failure of the corresponding genes to become transcriptionally upregulated during the implantation window. Thus, age-associated DNA methylation changes may underlie the decidualisation defects that are a common occurrence in older females. Alterations to the epigenome of uterine cells may therefore contribute significantly to the reproductive decline associated with advanced maternal age.

KEY WORDS: DNA methylation, Epigenetics, CpG islands, Reproduction, Ageing, Decidua

INTRODUCTION

Adaptation of the uterus to an implanting embryo is essential for a successful pregnancy. This process, termed decidualisation, is chiefly initiated by the ovarian steroid hormones oestrogen (E2) and progesterone (P4) (Wang and Dey, 2006; Adams and DeMayo, 2015). In response to this hormonal action, the uterus acquires a receptive state, ready to accept a blastocyst for implantation. Embryo attachment elicits a transformation of the primed uterine stromal cells to proliferate and then differentiate, which in the mouse typically results in the acquisition of a polyploid DNA content (Das et al., 1999). These hallmarks of the decidualisation reaction are accompanied by a swollen appearance of the uterus and an increase in uterine weight (Sharma et al., 2006; Lee et al., 2007).

We have recently shown that, in mice, this decidualisation reaction is markedly affected by maternal age (Woods et al., 2017).

Thus, advanced maternal age is associated with a dramatically attenuated decidualisation response, which is the main cause of the subsequent developmental problems observed in pregnancies of older females. This defect persists *in vitro* under optimal decidualisation conditions; uterine stromal cells isolated from older females exhibit a significantly slower or blunted response to E2 and P4 and fail to upregulate key marker genes of decidualisation such as *Bmp2*, *Hoxa10* and *Hand2*.

Ageing has been widely reported to correlate with changes in the DNA methylation landscape as a result of imperfect maintenance of DNA methylation marks (Issa, 2014). Consequently, sites that are normally heavily methylated lose methylation, and others that are unmethylated may gain some methylation (Pal and Tyler, 2016; Ciccarone et al., 2018). Generally, this loss of methylation fidelity results in the relative hypomethylation of retrovirally derived sequences, repeat elements and centromeres as well as loss of gene body methylation, whereas normally unmethylated CpG islands (CGIs) tend to acquire DNA methylation (Pal and Tyler, 2016; Ciccarone et al., 2018). Measuring DNA methylation at a few specific genomic sites can even predict chronological age in multiple tissues, including in the endometrium (Horvath, 2013; Olesen et al., 2017; Stubbs et al., 2017).

In the mouse, expression of the DNA methyltransferases *Dnmt1* and *Dnmt3a* increases at implantation sites between embryonic day (E) 4-8 (Gao et al., 2012). Both genes are also dramatically upregulated in artificially induced deciduomas, in which the hormonally primed uterus undergoes a decidualisation reaction in the absence of an implanting embryo. This upregulation of *de novo* and maintenance DNA methyltransferases suggests that DNA methylation may be an important epigenetic regulator of gene expression during decidualisation. In fact, inhibition of DNA methylation by 5-azacytidine treatment does not affect implantation but dramatically dampens the decidualisation response, with reduced uterine stromal cell proliferation and a failure to adequately upregulate decidualisation markers (Gao et al., 2012). This phenotype is similar to the abnormal decidualisation response we observed in aged pregnant females (Woods et al., 2017). This correlation in phenotypes raises the question of whether maternal ageing is accompanied by DNA methylation changes in the endometrium that have a negative impact on its capacity to decidualise.

Consequently, we set out to characterise the DNA methylation changes that take place in the endometrium as it differentiates to form the decidua during normal pregnancy, and to investigate the impact of advanced maternal age on the uterine and decidual epigenome.

RESULTS AND DISCUSSION
Expression and DNA methylation dynamics during decidualisation *in vivo*
To gain insight into the overall expression dynamics of epigenetic modifiers during decidualisation *in vivo*, we first analysed RNA-seq

[1]Epigenetics Programme, The Babraham Institute, Babraham Research Campus, Cambridge CB22 3AT, UK. [2]Centre for Trophoblast Research, University of Cambridge, Tennis Court Road, Cambridge CB2 3DY, UK. [3]Dept. of Cell Biology and Anatomy, Cumming School of Medicine, University of Calgary, Calgary, AB T2N 4N1, Canada. [4]Alberta Children's Hospital Research Institute, University of Calgary, Calgary, AB T2N 4N1, Canada. [5]Dept. of Biochemistry & Molecular Biology, Cumming School of Medicine, University of Calgary, Calgary, AB T2N 4N1, Canada. [6]Dept. of Medical Genetics, Cumming School of Medicine, University of Calgary, Calgary AB T2N 4N1, Canada.

*Author for correspondence (myriam.hemberger@ucalgary.ca)

M.H., 0000-0003-3332-6958

data from uterine samples during the implantation window at E3.5, and of dissected deciduas of E9.5, E10.5, E11.5 and E12.5 conceptuses developed in young control females (Woods et al., 2017). T-distributed stochastic neighbour embedding (t-SNE) analysis clustered the samples into four main groups, namely E3.5 uterus, E9.5 and E10.5 decidua, E11.5 decidua, and E12.5 decidua (Fig. 1A), showing the progression of transcriptional changes that accompany decidual development. As anticipated, the greatest transcriptomic differences were seen between the E3.5 and E12.5 time points (Fig. 1A). Among the differentially expressed genes were a number of epigenetic modifiers, notably those involved in DNA methylation dynamics (Fig. 1B). Most of these, including the ten-eleven translocation (Tet) enzymes, the DNA methylation maintenance surveillance factor *Uhrf1*, and multiple members of the methyl-CpG-binding domain (Mbd) family, were most highly

expressed at the early stages (E3.5 and E9.5) and declined towards the later stages of decidual maturation (E11.5-E12.5) (Fig. 1B). The DNA methyltransferases *Dnmt1*, *Dnmt3a* and *Dnmt3b* were transiently upregulated at E9.5, in line with previous observations (Gao et al., 2012). The most dramatic change was observed for *Tet1*, a 5-methylcytosine (5mC) dioxygenase enzyme involved in DNA demethylation, which was highly expressed at E3.5 but strongly downregulated thereafter.

The pronounced shift in expression of multiple factors involved in 5mC dynamics between the hormonally primed E3.5 uterus and later stages of decidualisation prompted us to compare the global DNA methylation landscapes at E3.5 and E11.5 in more detail, using DNA immunoprecipitation with a 5mC antibody followed by high-throughput sequencing (MeDIP-seq). When quantifying DNA methylation coverage in 2 kb tiling probes across the genome, the
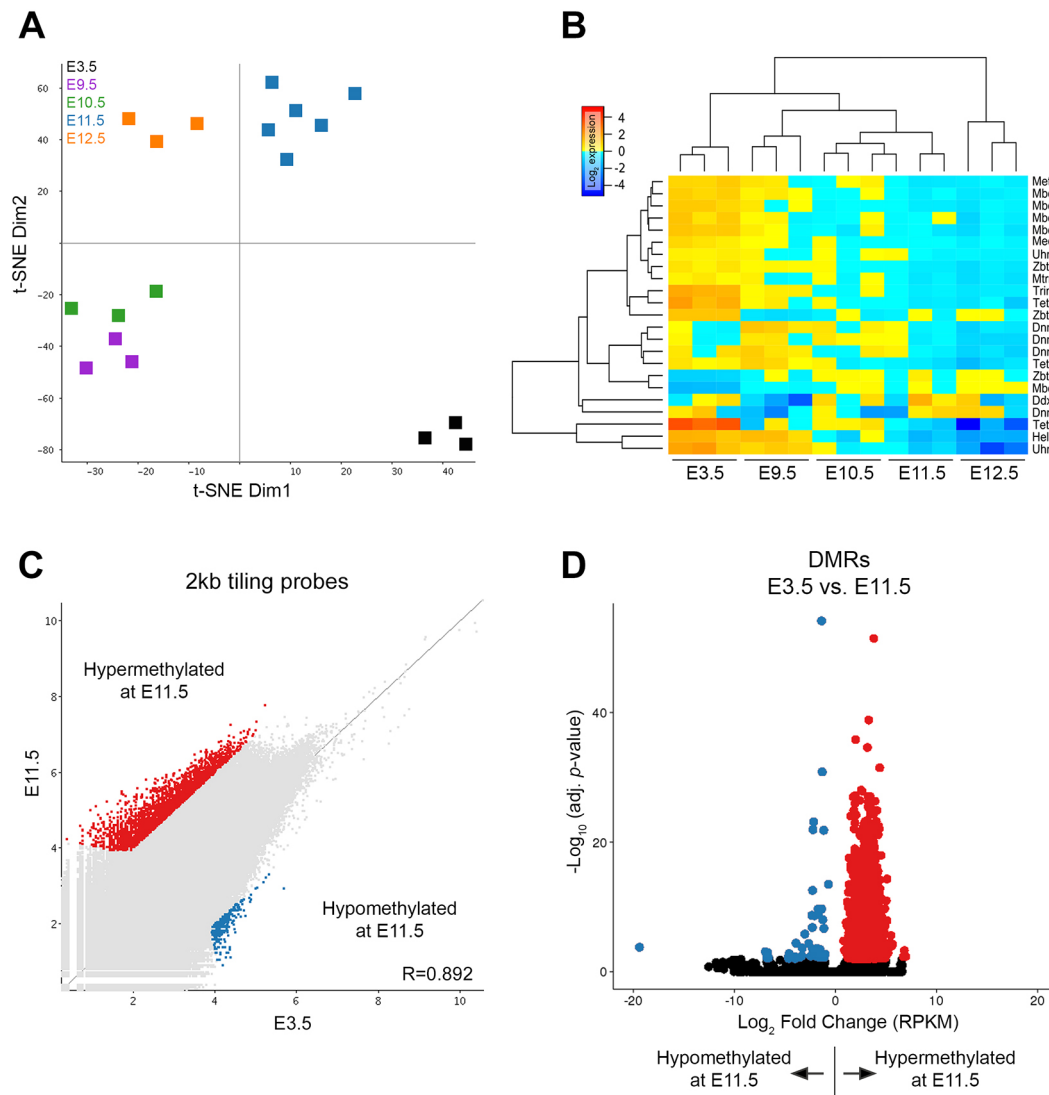

Fig. 1. Gene expression and DNA methylation dynamics during decidualisation. (A) t-SNE plot of RNA-seq data from E3.5 uteri (*n*=3) and decidual tissue at E 9.5 (*n*=3), E10.5 (*n*=3), E11.5 (*n*=6) and E12.5 (*n*=3). Developmental stages are characterised by expression signatures that cluster the samples into four groups: E3.5, (E9.5+E10.5), E11.5 and E12.5. (B) Heatmap depicting the expression profiles of epigenetic modifiers that are differentially expressed between E3.5 and E12.5. (C) Scatter plot of MeDIP-seq data of E3.5 uteri and E11.5 decidual samples (*n*=3 each). Each dot represents a 2 kb tiling probe, overlapping by 1 kb, covering the entire genome. Differentially enriched probes (Log₂ ±2) are colour-coded, with blue and red dots representing genomic regions that are hypo- and hypermethylated at E11.5, respectively. (D) Volcano plot of DMRs between E3.5 and E11.5 identified by MEDIPS analysis. The vast majority of DMRs gain methylation with the progression of decidualisation. Dots represent regions identified as potential DMRs by MEDIPS, with red and blue dots representing DMRs with adjusted *P*<0.05 and log-fold change >1 or <−1, respectively.

E3.5 and E11.5 samples exhibited very similar DNA methylation landscapes, as expected. However, a subset of regions were markedly differentially methylated, with the majority (90.6%) being hypermethylated at E11.5 (Fig. 1C). To better characterise the methylation changes between these stages, we used the MEDIPS program to identify genomic regions that exhibited significant differential methylation levels. This analysis revealed 8991 primary sequence stretches that exhibited a differential enrichment of 5mC, of which 8945 (99.5%) gained and 46 (0.5%) lost methylation between E3.5 and E11.5 (Fig. 1D). Merging of neighbouring tiles resulted in the identification of 3802 differentially methylated regions (DMRs) between E3.5 and E11.5 (Table S1) that were used for further analysis.

Differentially methylated regions are enriched at decidualisation genes

The identified DMRs were predominantly located in distal intergenic regions (∼50%), defined as >3 kb upstream or downstream of the nearest gene. Approximately 40% were in introns and 5% at promoter regions (Fig. 2A). Interestingly, analysis with the Genomic Regions Enrichment of Annotations Tool (GREAT) indicated an association of the identified DMRs with genes related to proliferation, growth and endometrial maturation (Fig. 2B). This included terms related to the regulation of stem cell maintenance, TGFβ-, NODAL-, VEGF- and WNT-signalling, and mesenchymal-to-epithelial transition, a well-characterised process in the later stages of decidualisation (Patterson et al., 2013; Zhang et al., 2013; Yu et al., 2016). Genes involved in the regulation of cholesterol transport, a substrate required for the synthesis of E2 and P4, and E2-signalling pathway components, were also enriched for DMRs and may therefore be subject to regulation by DNA methylation during decidualisation.

Integrating the methylome and transcriptome datasets revealed that a significant proportion (36%) of DMRs overlapping or upstream of a gene (within ≤5 kb upstream of a transcription start site or ≥1 bp overlap with a gene) were associated with
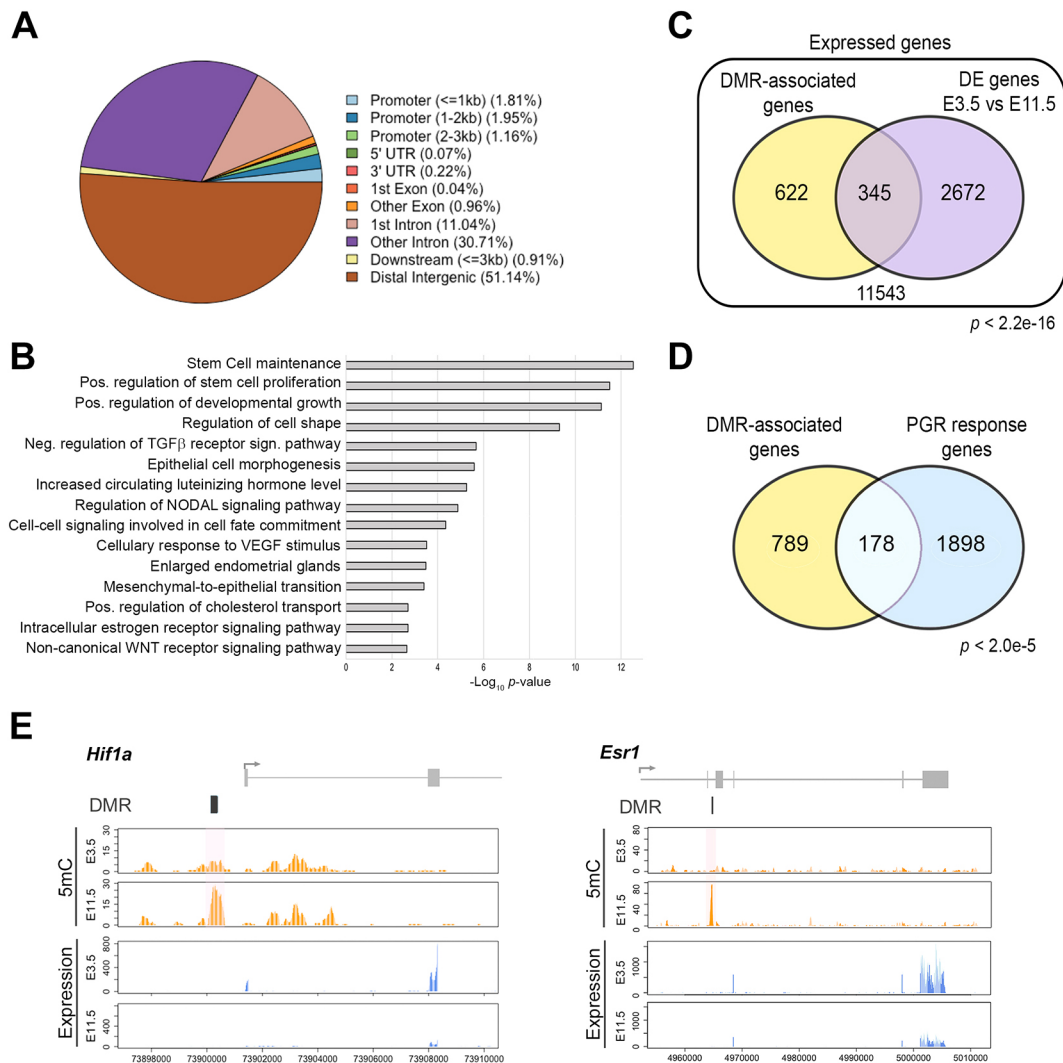

Fig. 2. Genomic characterisation of decidualisation DMRs. (A) Genomic distribution of DMRs identified by comparing E3.5 uteri with E11.5 decidual MeDIP-seq samples using MEDIPS analysis. (B) Gene ontology and mammalian phenotype terms associated with the identified DMRs. Terms with specific relevance to pregnancy and decidualisation are shown. (C) Overlap of genes associated with a DMR (defined as ≥1 bp overlap between DMR and gene or DMR ≤5 kb upstream of transcription start site) and differentially expressed (DE) genes between E3.5 uteri and E11.5 decidua. DE genes were limited to expression differences with a log-fold change of ±2. (D) Intersection of genes associated with a DMR (defined as above) and differentially expressed genes between wild-type (WT) and progesterone receptor (Pgr) knockout uteri (Jeong et al., 2005). (E) Examples of the Hif1a and Esr1 gene loci where a gain of DNA methylation (5mC) at identified DMRs (shaded) correlates with lower gene expression at E11.5 compared with E3.5. Wiggle plots of read count enrichments across these regions are shown.

differentially expressed transcripts between E3.5 and E11.5 (Fig. 2C). This considerable overlap may suggest that DNA methylation changes laid down during pregnancy progression contribute to the transcriptional regulation of these genes. This regulation may be directed through the action of the progesterone receptor (PGR), as a significant proportion of genes associated with a DMR were also affected by *Pgr* ablation (Fig. 2D; Jeong et al., 2005). Notably, hypermethylated DMRs were found at genes with known roles in placental development and decidualisation. For example, DMRs that gain methylation over gestation were detected in the promoter region of the P4-regulated gene *Hif1a* and within introns of the oestrogen receptor *Esr1*, the cyclase-associated actin cytoskeleton regulatory protein *Cap2* and the immunophilin *Fkbp5*, which acts as a chaperone for PGR (Fig. 2E; Fig. S1). In all of these cases, the increased methylation at the identified DMRs correlated with decreased gene expression at later stages of decidualisation, suggesting that the intron methylation affects gene regulatory enhancer elements at these loci.

Overall, our approaches identified a set of uterine DMRs that overwhelmingly gain DNA methylation in the decidua during gestation. These DMRs are significantly associated with decidualisation genes, in particular those regulated by P4. This is consistent with previous reports that showed an increase in DNA methyltransferase expression after implantation (Gao et al., 2012). These data imply that a cohort of P4-responsive decidualisation genes are epigenetically regulated; after their initial transcriptional burst during early stages of decidualisation, they are methylated and repressed in mature decidual cells during later stages of gestation. This finding is in line with the reported failure in the progression of decidualisation upon exposure to the DNA methylation inhibitor 5-azacytidine (Gao et al., 2012).

Altered methylation dynamics may underlie age-associated decidualisation defects

The enrichment of DMRs at P4-regulated genes was of particular interest as these genes are highly sensitive to age-related changes (Woods et al., 2017). To assess whether alterations to the DNA methylation profile may affect the regulation of these genes and thereby account for the decidualisation defect of older females, we performed the MeDIP-seq analysis also on E3.5 uterine and E11.5 decidual samples from females aged 41-49 weeks. Overall, the methylation dynamics were very similar in the aged samples compared with young, with most changes entailing a gain of methylation between E3.5 and E11.5 at the vast majority of differentially enriched loci (5198/5610; 93%) (Fig. S2A). The 5mC enrichment distribution across various genomic features was also globally very similar (Fig. S2B). Contrary to the well-reported loss of gene body methylation as a function of age, no statistically significant difference was detected between young and aged uterine and decidual samples across gene bodies. However, an exception to this overall similarity was evident at CGIs that exhibited globally higher DNA methylation levels in the aged samples (Fig. S2B).

We thus turned our attention specifically to CGI methylation changes. When comparing the E3.5 and E11.5 developmental stages within each age group, we identified 302 and 1212 differentially methylated CGIs in the young and aged samples, respectively. As observed with the whole genome-covering probes, the majority of these developmentally dynamic CGIs gained methylation with the progression of decidualisation in both young and aged samples (Fig. S2C). However, the overall gain of 5mC was more pronounced in the aged cohort (Fig. S2C), resulting in the greater number of differentially enriched CGIs in aged than in

young samples. CGIs are therefore the genomic feature most susceptible to methylation changes during reproductive ageing.

Intriguingly, the most conspicuous difference was observed when assessing the smaller fraction of developmentally dynamic CGIs that lose methylation during the progression of decidualisation. This cohort of CGIs was far more highly 5mC-enriched in aged than in young E3.5 uteri (Fig. S2C). Directly comparing CGI methylation of E3.5 young and aged samples revealed 41 differentially methylated CGIs, 40 of which were hypermethylated in aged samples (Fig. 3A). We independently verified the differential methylation pattern at the *Fzd2* CGI by bisulphite sequencing (Fig. S2D). When assessing whether promoter-associated differentially methylated CGIs affected expression of the corresponding genes (Woods et al., 2017), we found that 75% of these genes were downregulated in aged samples (Fig. 3B). This included pivotal regulators of decidualisation, notably the WNT receptor *Fzd2* and the *Hoxa10/Hoxa11* gene cluster (Fig. 3C,D; Fig. S3A, Table S3) (Hsieh-Li et al., 1995; Benson et al., 1996; Lim et al., 1999; Hayashi et al., 2009). Thus, age-associated CGI hypermethylation likely prevents the induction of these genes to achieve normal expression levels during early decidualisation.

CGI hypermethylation was correlated with a significant downregulation of *Tet1* expression in E3.5 uteri of aged females compared with young (Fig. 3E, Fig. S3B, Tables S3 and S4). These lower *Tet1* levels corresponded with a strikingly reduced staining intensity for 5-hydroxymethylcytosine (5hmC) in aged uteri, specifically in glandular epithelial cells (Fig. 3F). Although 5mC staining intensities were not appreciably altered or only mildly increased in aged samples by visual inspection, we observed significant changes in the ground state expression of the DNA methylation machinery components *Dnmt1*, *Dnmt3b*, *Uhrf1* and *Trim28* (also known as *Kap1*), which were all expressed at significantly higher levels in uterine stromal cells from aged compared with young females (Fig. S3C). Collectively, this deregulation of epigenetic modifiers may well account for the gain in CGI methylation that is evident in the uteri of aged females, and may be a major contributor to the frequent developmental demise of embryos in these pregnancies.

Taken together, in the temporal context of reproductive ageing, early epigenetic changes seem to affect CGI methylation specifically whereas other epigenetic hallmarks of organismal ageing, such as loss of gene body methylation, are not yet evident. We find that a number of CGIs at crucial decidualisation genes are hypermethylated at E3.5 in aged female uteri, which may interfere with appropriate gene induction thus impeding the progression of early postimplantation development. The most prominent examples of genes with differentially methylated promoter CGIs were *Hoxa10*, *Hoxa11* and *Fzd2*. *Hoxa11* deficiency causes a hypoplastic uterine phenotype with fewer glands whereas *Hoxa10* ablation causes reduced stromal cell proliferation and overall decidualisation failure, with both knockouts resulting in female infertility (Hsieh-Li et al., 1995; Satokata et al., 1995; Benson et al., 1996; Lim et al., 1999). WNT signalling through FZD receptors is also highly dynamically regulated during decidualisation and has important roles in supporting this cellular transformation process (Hayashi et al., 2009). Overall, here we show that the uterine epigenome of older females undergoes age-related alterations that likely interfere with the robust response to steroid hormones required for normal decidualisation. These epigenetic changes may explain the significant decidualisation defects and consequent developmental failures associated with declining reproduction in older female mice. Although it may be tempting to speculate that treatment with methylation inhibitors such as 5-azacytidine could prevent or reset
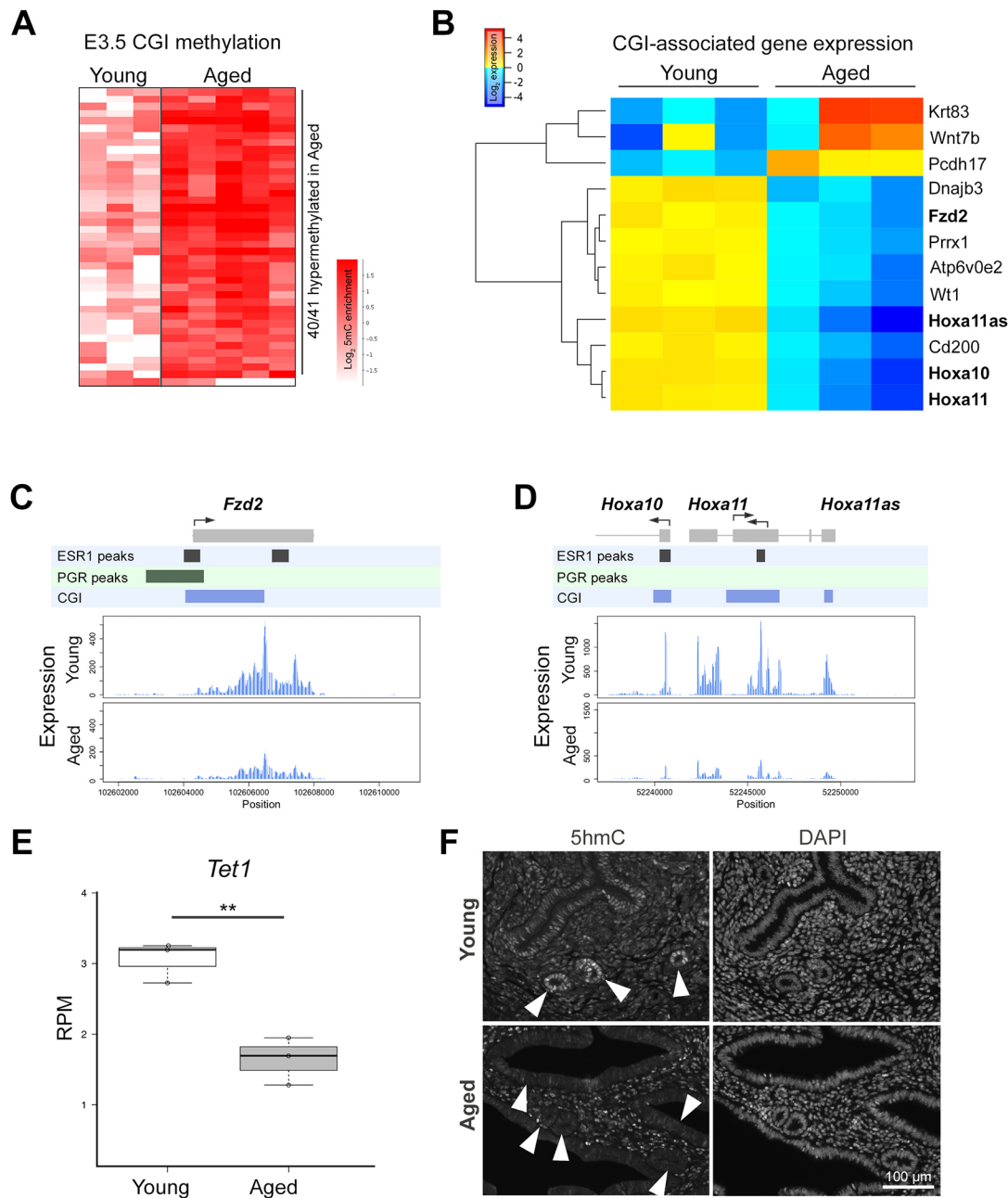
Fig. 3. Ageing-induced DNA methylation changes may interfere with decidualisation. (A) Heatmap of differentially methylated CpG islands (CGIs) identified by comparing E3.5 uteri from young (*n*=3) and aged (*n*=5) females. (B) Heatmap displaying expression levels of genes associated with promoter-associated differentially methylated CGIs. Expression data are of E3.5 uteri from young and aged females (Woods et al., 2017). (C) Genome browser view of the *Fzd2* locus, which contains a promoter-associated CGI that is hypermethylated in aged E3.5 uteri compared with young (indicated by blue bars). ESR1- and PGR-binding sites are also shown. The wiggle plot depicts read counts of RNA-seq data (merged of *n*=3 each). (D) Genome browser view as in C of the *Hoxa10/11* gene cluster. (E) Box plot of *Tet1* gene expression levels in E3.5 uteri of young and aged females, determined by RNA-seq (RPM, reads per million). Centre lines show medians; box limits indicate 25th and 75th percentiles and whiskers extend 1.5× the interquartile range from the 25th and 75th percentiles. **$P<0.01$ (Student's *t*-test; one-tailed, unpaired). (F) Immunofluorescence staining for 5-hydroxymethylcytosine (5hmC) on cross-sections of E3.5 uteri from young and aged females, performed on three biological replicates. Nuclei were counterstained with DAPI. Arrowheads point to uterine glands and/or the luminal epithelium. 5hmC staining is particularly higher in glandular epithelial cells of young uteri compared with aged.

some of these changes, the difficulty will be to direct them to the correct target loci. However, since DNA methylation changes also correlate with gene expression dynamics in the human endometrium during the endometrial cycle (Kukushkina et al., 2017), such age-induced epigenomic rearrangements may be of significant importance for the decline in uterine function and fertility linked to advanced maternal age in humans.

MATERIALS AND METHODS

Mice

husbandry practice guidelines, under 12 h light-dark cycles. Mice were fed CRM (P) diet (Special Diet Services) *ad libitum* and received seeds (e.g. sunflower or millet) as part of their environmental enrichment. 'Young' females were 8-20 weeks old and 'Aged' females were 41-49 weeks old. Timed matings were set up between virgin females and stud males of 8-16 weeks of age, counting the morning of the vaginal plug as E0.5. Pregnant females were dissected at the gestational age indicated.

RNA/DNA isolation, RT-qPCR and bisulphite sequencing
RNA and DNA were isolated simultaneously from whole frozen tissue using the AllPrep DNA/RNA Mini Kit (Qiagen, 80204). RNA from uterine stromal cells was isolated using TRI Reagent (Sigma-Aldrich, T9424), following the manufacturer's instructions. For RT-qPCR, RNA was reverse transcribed using RevertAid H Minus Reverse Transcriptase (ThermoFisher, EP0451) to generate cDNA and PCRs performed using QuantiNova SYBR Green PCR Kit (Qiagen, 208056) on a Bio-Rad CFX96 cycler. Bisulphite conversion was performed with the EpiTect Bisulfite Kit (Qiagen, 59104) according to the manufacturer's instructions. PCR products were cloned into the pGEM-T Easy Vector System (Promega, A1360) and then sequenced. Primer sequences are provided in Table S2.

Cell culture
Uterine stromal cells were isolated largely as previously described (Afonso et al., 2002). In brief, uteri from E3.5 mice were slit longitudinally and disaggregated with 2.5% pancreatin (Sigma-Aldrich, P3293) and 0.5% trypsin (type III) (Sigma-Aldrich, T4799) in Hank's balanced salt solution (HBSS). After vortexing, the medium was removed and the remaining tissue was washed twice in HBSS (discarding luminal epithelial cells) and incubated for 30 min at 37°C in HBSS containing 0.007% collagenase (Thermo Fisher Scientific, 17104-019), 0.02% DNase I (Roche, 10104159001) and 0.008% protease (Sigma-Aldrich, P8811) with vortexing every 5 min. Dissociated tissues were then triturated, filtered through a 70 μm cell strainer (BD Biosciences) and spun at 1000 g for 5 min at 4°C. Cell pellets were resuspended in phenol-red free Dulbecco's modified Eagle's medium: Nutrient Mixture F-12 (DMEM/F-12) (Thermo Fisher Scientific, 21041-025) plus 10% foetal bovine serum, 1 mM sodium pyruvate (Thermo Fisher Scientific, 11360-039), 1× antimycotic/ antibiotic (Thermo Fisher Scientific, 15240-062) and 50 μM 2-mercaptoethanol (Thermo Fisher Scientific, 31350-010).

RNA sequencing
RNA-seq libraries were generated using the SureSelect Strand-Specific RNA Library Preparation kit (Agilent, G9691A) or the ScriptSeq V2 RNA-seq Library Preparation Kit (Illumina, SSV21124). Libraries were quality-controlled using the Bioanalyzer 2100 (Agilent) and quantified using the KAPA Library Quantification Kit (KAPA Biosystems, KK4824). Indexed libraries were pooled and sequenced on an Illumina HiSeq2500 sequencer, using a 100 bp single-end protocol. FastQ data were trimmed for adaptors using Trim Galore! v0.4.4, before mapping to the *Mus musculus* GRCm38 genome assembly using HISAT2 v2.1.0 (uterine stromal cells), or TopHat v2.0.12 (whole uterus and decidua). Data were quantified using the RNA-seq quantitation pipeline in SeqMonk (www.bioinformatics.babraham.ac. uk), and normalised according to total read count (read per million mapped reads, RPM). Differential expression was calculated using DESeq2 with $P<0.05$ and adjusted for multiple testing correction using the Benjamini–Hochberg method. For stringent difference analysis, an intensity difference filter of ±2 (after log transformation) was applied in SeqMonk. *Pgr* KO expression data were retrieved from NCBI Gene Expression Omnibus (www.ncbi.nlm.nih.gov/geo/query/acc.cgi?acc=GSE39920).

MeDIP sequencing
Sonicated DNA (1.5 μg) was subjected to methylated DNA immunoprecipitation (MeDIP) as described previously (Senner et al., 2012). Indexed libraries were pooled and sequenced on an Illumina HiSeq2500 sequencer, using a 50 bp paired-end protocol. FastQ data were trimmed and aligned to the *Mus musculus* GRCm38 genome assembly using Bowtie v2.3.2. DMRs were identified by either the MEDIPS package in R, using a window size of 200 bp and Bonferroni P-value cut-off of 0.01,

or using LIMMA statistics with $p_{Bonf}<0.05$ for replicated datasets within SeqMonk. To detect meaningful enrichment differences, minimum read count cut-offs were set per probe and sample set: for 2 kb running windows ≥10 reads per probe, and for CGIs ≥5 reads per probe in at least one of the replicate sample sets. Neighbouring windows were merged, and those located in blacklist regions were removed (ENCODE project, accession ENCSR636HFF). The feature distribution of DMRs was determined using ChIPseeker in R. The enrichment of methylated fragments in different genomic features was determined by dividing the number of reads in each feature by the percentage of the genome occupied by that feature, followed by log transformation.

Bioinformatic tools and statistics
Heatmaps were generated using heatmap.2 in R. Principal component analysis was performed using DESeq2 rlog-normalised RNA-seq data on read counts using the top 500 most variable genes. The principal component analysis results were plotted using prcomp in R. t-SNE plots were generated using SeqMonk (www.bioinformatics.babraham.ac.uk).

Volcano plots and wiggle plots were generated in R using ggplot2 and core R plotting functionality, respectively. Gene Ontology (GO) and gene set enrichment analyses using the MSigDB (software.broadinstitute.org/ gsea/msigdb) were performed on genes found to be significantly differentially upregulated or downregulated, against a background list of genes consisting of those with more than ten reads aligned. GO terms with a Bonferroni P-value of <0.05 were found using DAVID (Huang da et al., 2009) and GREAT (McLean et al., 2010). Venn diagrams were plotted using BioVenn (www.cmbi.ru.nl/cdd/biovenn/). Two-way ANOVA and Fisher's exact test were performed using GraphPad Prism and R, respectively.

5hmC staining
E3.5 uteri of young and aged females were fixed in 4% paraformaldehyde, processed for routine paraffin histology and embedded in the same paraffin block. Sections (7 μm thick) were used for staining. Sections were deparaffinised and rehydrated according to standard protocols. A denaturation step was performed using 2N HCl for 20-40 min. Sections were blocked in PBS, 0.1% Tween 20 and 0.5% Bovine Serum Albumin, and incubated with an anti-5hmC antibody (Active Motif, 39769; 1:1000). Detection was carried out with the appropriate Alexa Fluor 488-conjugated secondary antibody (1:600; Life Technologies, A-21206). Nuclear counterstaining was performed with 4′,6-diamidine-2′-phenylindole dihydrochloride (DAPI) (MilliporeSigma, 10236276001). Images were captured using an Olympus BX41 Fluorescence Microscope.

Source data
Source data for Fig. S3A,B and Fig. 3E are provided in Tables S3 and S4, respectively.

Competing interests
The authors declare no competing or financial interests.

Author contributions
Conceptualization: L.W., M.H.; Methodology: L.W., N.M., V.P.-G., W.D., M.H.; Software: L.W.; Validation: L.W., N.M., X.Z., W.D., V.P.-G.; Formal analysis: L.W., M.H.; Investigation: L.W., N.M., X.Z., W.D., V.P.-G.; Writing - original draft: L.W., M.H.; Writing - review & editing: W.D., M.H.; Visualization: L.W., M.H.; Supervision: W.D., M.H.; Project administration: M.H.; Funding acquisition: M.H.

DEVELOPMENT

Data availability

High-throughput sequencing data have been deposited in Gene Expression Omnibus under accession numbers GSE138375 for the MeDIP data; GSE98901 for RNA-seq data of developmental time course of decidualisation, E3.5 uteri and E11.5 decidua; and GSE138375 for RNA-seq data of uterine stromal cells.

Supplementary information

Supplementary information available online at
http://dev.biologists.org/lookup/doi/10.1242/dev.185629.supplemental

References

Adams, N. R. and DeMayo, F. J. (2015). The role of steroid hormone receptors in the establishment of pregnancy in rodents. *Adv. Anat. Embryol. Cell Biol.* **216**, 27-49. doi:10.1007/978-3-319-15856-3_3

Afonso, S., Tovar, C., Romagnano, L. and Babiarz, B. (2002). Control and expression of cystatin C by mouse decidual cultures. *Mol. Reprod. Dev.* **61**, 155-163. doi:10.1002/mrd.1142

Benson, G. V., Lim, H., Paria, B. C., Satokata, I., Dey, S. K. and Maas, R. L. (1996). Mechanisms of reduced fertility in Hoxa-10 mutant mice: uterine homeosis and loss of maternal Hoxa-10 expression. *Development* **122**, 2687-2696.

Ciccarone, F., Tagliatesta, S., Caiafa, P. and Zampieri, M. (2018). DNA methylation dynamics in aging: how far are we from understanding the mechanisms? *Mech. Ageing Dev.* **174**, 3-17. doi:10.1016/j.mad.2017.12.002

Das, S. K., Lim, H., Paria, B. C. and Dey, S. K. (1999). Cyclin D3 in the mouse uterus is associated with the decidualization process during early pregnancy. *J. Mol. Endocrinol.* **22**, 91-101. doi:10.1677/jme.0.0220091

Gao, F., Ma, X., Rusie, A., Hemingway, J., Ostmann, A. B., Chung, D. and Das, S. K. (2012). Epigenetic changes through DNA methylation contribute to uterine stromal cell decidualization. *Endocrinology* **153**, 6078-6090. doi:10.1210/en.2012-1457

Hayashi, K., Erikson, D. W., Tilford, S. A., Bany, B. M., Maclean, J. A., II, Rucker, E. B., III, Johnson, G. A. and Spencer, T. E. (2009). Wnt genes in the mouse uterus: potential regulation of implantation. *Biol. Reprod.* **80**, 989-1000. doi:10.1095/biolreprod.108.075416

Horvath, S. (2013). DNA methylation age of human tissues and cell types. *Genome Biol.* **14**, R115. doi:10.1186/gb-2013-14-10-r115

Hsieh-Li, H. M., Witte, D. P., Weinstein, M., Branford, W., Li, H., Small, K. and Potter, S. S. (1995). Hoxa 11 structure, extensive antisense transcription, and function in male and female fertility. *Development* **121**, 1373-1385.

Huang da, W., Sherman, B. T. and Lempicki, R. A. (2009). Systematic and integrative analysis of large gene lists using DAVID bioinformatics resources. *Nat. Protoc.* **4**, 44-57. doi:10.1038/nprot.2008.211

Issa, J. P. (2014). Aging and epigenetic drift: a vicious cycle. *J. Clin. Invest.* **124**, 24-29. doi:10.1172/JCI69735

Jeong, J.-W., Lee, K. Y., Kwak, I., White, L. D., Hilsenbeck, S. G., Lydon, J. P. and DeMayo, F. J. (2005). Identification of murine uterine genes regulated in a ligand-dependent manner by the progesterone receptor. *Endocrinology* **146**, 3490-3505. doi:10.1210/en.2005-0016

Kukushkina, V., Modhukur, V., Suhorutšenko, M., Peters, M., Mägi, R., Rahmioglu, N., Velthut-Meikas, A., Altmäe, S., Esteban, F. J., Vilo, J. et al. (2017). DNA methylation changes in endometrium and correlation with gene expression during the transition from pre-receptive to receptive phase. *Sci. Rep.* **7**, 3916. doi:10.1038/s41598-017-03682-0

Lee, K. Y., Jeong, J.-W., Tsai, S. Y., Lydon, J. P. and DeMayo, F. J. (2007). Mouse models of implantation. *Trends Endocrinol. Metab.* **18**, 234-239. doi:10.1016/j.tem.2007.06.002

Lim, H., Ma, L., Ma, W.-G., Maas, R. L. and Dey, S. K. (1999). Hoxa-10 regulates uterine stromal cell responsiveness to progesterone during implantation and decidualization in the mouse. *Mol. Endocrinol.* **13**, 1005-1017. doi:10.1210/mend.13.6.0284

McLean, C. Y., Bristor, D., Hiller, M., Clarke, S. L., Schaar, B. T., Lowe, C. B., Wenger, A. M. and Bejerano, G. (2010). GREAT improves functional interpretation of cis-regulatory regions. *Nat. Biotechnol.* **28**, 495-501. doi:10.1038/nbt.1630

Olesen, M. S., Starnawska, A., Bybjerg-Grauholm, J., Bielfeld, A. P., Agerholm, I. E., Forman, A., Overgaard, M. T. and Nyegaard, M. (2017). Biological age of the endometrium using DNA methylation. *Reproduction* **155**, 165-170. doi:10.1530/REP-17-0601

Pal, S. and Tyler, J. K. (2016). Epigenetics and aging. *Sci. Adv.* **2**, e1600584. doi:10.1126/sciadv.1600584

Patterson, A. L., Zhang, L., Arango, N. A., Teixeira, J. and Pru, J. K. (2013). Mesenchymal-to-epithelial transition contributes to endometrial regeneration following natural and artificial decidualization. *Stem Cells Dev.* **22**, 964-974. doi:10.1089/scd.2012.0435

Satokata, I., Benson, G. and Maas, R. (1995). Sexually dimorphic sterility phenotypes in Hoxa10-deficient mice. *Nature* **374**, 460-463. doi:10.1038/374460a0

Senner, C. E., Krueger, F., Oxley, D., Andrews, S. and Hemberger, M. (2012). DNA methylation profiles define stem cell identity and reveal a tight embryonic-extraembryonic lineage boundary. *Stem Cells* **30**, 2732-2745. doi:10.1002/stem.1249

Sharma, S., Murphy, S. P. and Barnea, E. R. (2006). Genes regulating implantation and fetal development: a focus on mouse knockout models. *Front. Biosci.* **11**, 2123-2137. doi:10.2741/1955

Stubbs, T. M., Bonder, M. J., Stark, A.-K., Krueger, F., Team, B. I. A. C., von Meyenn, F., Stegle, O. and Reik, W. (2017). Multi-tissue DNA methylation age predictor in mouse. *Genome Biol.* **18**, 68. doi:10.1186/s13059-017-1203-5

Wang, H. and Dey, S. K. (2006). Roadmap to embryo implantation: clues from mouse models. *Nat. Rev. Genet.* **7**, 185-199. doi:10.1038/nrg1808

Woods, L., Perez-Garcia, V., Kieckbusch, J., Wang, X., DeMayo, F., Colucci, F. and Hemberger, M. (2017). Decidualisation and placentation defects are a major cause of age-related reproductive decline. *Nat. Commun.* **8**, 352. doi:10.1038/s41467-017-00308-x

Yu, J., Berga, S. L., Johnston-MacAnanny, E. B., Sidell, N., Bagchi, I. C., Bagchi, M. K. and Taylor, R. N. (2016). Endometrial stromal decidualization responds reversibly to hormone stimulation and withdrawal. *Endocrinology* **157**, 2432-2446. doi:10.1210/en.2015-1942

Zhang, X.-H., Liang, X., Liang, X.-H., Wang, T.-S., Qi, Q.-R., Deng, W.-B., Sha, A.-G. and Yang, Z.-M. (2013). The mesenchymal-epithelial transition during in vitro decidualization. *Reprod. Sci.* **20**, 354-360. doi:10.1177/1933719112472738